Effect of initial fluctuations on the collective flow in intermediate-energy heavy ion collisions

J. Wang (王佳),[1,2] Y. G. Ma (马余刚),[1,3,*] G. Q. Zhang (张国强),[1] and W. Q. Shen (沈文庆)[1,3]
[1]*Shanghai Institute of Applied Physics, Chinese Academy of Sciences, Shanghai 201800, China*
[2]*University of Chinese Academy of Sciences, Beijing 100049, China*
[3]*Shanghai Tech University, Shanghai 200031, China*
(Received 1 August 2014; published 4 November 2014)

A systemical analysis of the initial fluctuation effect on the collective flows for Au + Au at 1*A* GeV is presented in the framework of isospin-dependent quantum molecular dynamics model (IQMD), and a special focus on the initial fluctuation effect on the squeeze out is emphasized. The flows calculated by the participant plane reconstructed by the initial geometry in coordinate space are compared with those calculated by both the ideal reaction-plane and event-plane methods. It is found that initial fluctuation weakens the squeeze-out effect, and some discrepancies between the flows extracted by these different plane methods appear, which indicate that the flows are affected by the evolution of dynamics. In addition, we find that the squeeze-out flow is also proportional to initial eccentricity. Our calculations also qualitatively give a trend for the excitation function of the elliptic flow similar to that of the FOPI Collaboration experimental data. Finally, we address the nucleon number scaling of the flows for light particles. Even though the initial fluctuation significantly decreases the ratio v_4/v_2^2 and $v_3/(v_1v_2)$, all fragments to mass number 4 keep the same curve and show independence from transverse momentum.

DOI: 10.1103/PhysRevC.90.054601 PACS number(s): 25.75.Ld, 02.70.Ns, 24.10.Lx

I. INTRODUCTION

Recent relativistic heavy ion collision (HIC) studies have recognized the importance of the initial fluctuations on the various order of flows [1–13]. For instance, the origin of the triangular flow v_3 and higher harmonics is fluctuation in initial conditions [5,9,14]. In particular, v_3 vanishes, if the system starts with a smooth almond-shaped initial state [5]. It also shows that the ratio of elliptic flow to eccentricity (v_2/ε_2) is sensitive to the initial fluctuation. By now, studies on the initial fluctuation effects are only limited in relativistic heavy ion collisions. At these energies, the initial fluctuation can be followed by hydrodynamic expansion and result in the long-range azimuthal correlations (or the anisotropy flows). Its energy dependence is thought to be one of the important observables to study various aspects of the QCD phase diagram in the beam-energy scan (BES) program at the BNL Relativistic Heavy Ion Collider (RHIC) [15–18]. In intermediate-energy HICs, no systematic study for the initial-fluctuation effects on the collective flow has been presented except for a brief report that appeared by the same authors of the present work [19]. Also, the relationship between the eccentricity and squeeze out (negative elliptic flow) is not yet reported to our knowledge. In contrast with relativistic-energy HICs, the timescale of collision dynamics is larger (from tens of fm/c to hundreds of fm/c) in intermediate-energy HICs, which may allow the other factors to develop and smear the long-range azimuthal correlations originating from the initial fluctuation. It is then worth addressing how the initial fluctuation affects the collective flow in the intermediate-energy domain.

In this paper, the collective flows are calculated within a framework of a nuclear transport model; namely isospin quantum molecular dynamics (IQMD), which allows the generation of events with event-by-event-fluctuating initial conditions. To explore the effects of the initial fluctuation, we study the flows as functions of centrality, transverse component of four velocity, and rapidity. Flow results with respect to different reaction-plane determinations are compared with the experimental data. We also try to reproduce experimental excitation functions of elliptic flow with our simulations. In addition, the relationship of elliptic flow versus eccentricity is discussed in different centralities. The dependence of the collective flow on the equation of state (EOS) is also presented. At the end, we focus on the phenomenology of the mass-number-scaling behavior of different harmonic flows and check the initial-fluctuation effect on scaling behavior.

The paper is organized in the following way: A brief description of the IQMD model is introduced in Sec. II. The initial fluctuation is described in Sec. III. The methodology of the flow calculations is presented in Sec. IV. The results and discussion are presented in Sec. V. Finally, a summary is given in Sec. VI.

II. BRIEF DESCRIPTION OF ISOSPIN QUANTUM MOLECULAR DYNAMICS

The quantum molecular dynamics (QMD) approach is an n-body theory to simulate heavy ion reactions at intermediate energies. It contains several major parts: the initialization of the target and the projectile nucleons, the spread of nucleons in the effective potential, the collisions between the nucleons, and the Pauli-blocking effect [20]. There are different versions of QMD which are best used in different energy regions [21–25]. Of these, the IQMD model is based on the QMD model and takes the isospin effects into account in various aspects: a different density distribution for neutrons and protons, the asymmetric potential term of the mean field, and

*ygma@sinap.ac.cn

the use of experimental cross sections for nucleon-nucleon and Pauli-blocking for neutron and proton, respectively [21,22].

In IQMD each nucleon is represented by a Gaussian wave packet with a width parameter (here $L = 8.66$ fm^2) centered around the mean position $\vec{r}_i(t)$ and mean momentum $\vec{p}_i(t)$ [26,27]:

$$\phi_i(\vec{r},t) = \frac{1}{(2\pi L)^{3/4}} \exp\left[-\frac{[\vec{r}-\vec{r}_i(t)]^2}{4L}\right] \exp\left[-\frac{i\vec{r}\cdot\vec{p}_i(t)}{\hbar}\right]. \tag{1}$$

The nucleons interact by means of the nuclear mean field and nucleon-nucleon collisions. The nuclear mean field can be written as

$$U(\rho,\tau_z) = \alpha\left(\frac{\rho}{\rho_0}\right) + \beta\left(\frac{\rho}{\rho_0}\right)^{\gamma} + \delta \ln^2[\varepsilon(\Delta p)^2 + 1]\left(\frac{\rho}{\rho_0}\right) + \frac{1}{2}(1-\tau_z)V_c\frac{(\rho_n-\rho_p)}{\rho_0}\tau_z + U^{\text{Yuk}}, \tag{2}$$

where ρ_0 is the normal nuclear matter density (here $\rho_0 = 0.17$ fm^{-3}), ρ_n and ρ_p are the total neutron and proton densities respectively, τ_z is zth component of the isospin degree of freedom, which equals 1 or -1 for neutrons or protons, respectively. The coefficients α, β, and γ are the Skyrme parameters, which connect closely with the EOS of bulk nuclear matter. Two of them are fixed by the constraints that the total energy is a minimum at the saturation density $\rho = \rho_0$ with a value of $E/A = -16$ MeV which corresponds to the volume energy in the Bethe–Weizsäcker mass formula and the free particle without binding energy. The third parameter is fixed by the nuclear compressibility, which is defined by

$$\kappa = 9\rho^2\frac{\partial^2}{\partial\rho^2}\left(\frac{E}{A}\right). \tag{3}$$

Two different equations of state are commonly used: a hard equation of state (H) with a compressibility of $\kappa = 380$ MeV and a soft equation of state (S) with a compressibility of $\kappa = 200$ MeV [28–30]. δ and ε are the optional coefficients for the momentum-dependent potential, which are taken from the measured energy dependence of the proton-nucleus optical potential [22]. HM and SM mean the hard equation of state and soft equation of state with momentum-dependent potential. C_{sym} is the symmetry-energy strength due to the difference of neutron and proton. V_c is the Coulomb potential and U^{Yuk} is the Yukawa potential.

For the collisions, IQMD uses the experimental cross section which contains the isospin effects and nuclear-medium effect [22]. Pauli blocking is also considered after the collisions to consider the fermion property of nucleons.

In IQMD initialization, the centroid of the Gaussian in a nucleus is randomly distributed in a phase space sphere ($r \leqslant R$ and $p \leqslant p_F$) with $R = 1.12A^{1/3}$ fm corresponding to a ground-state density of $\rho_0 = 0.17$ fm^{-3} [31]. P_F is the Fermi momentum, which depends on the ground-state density. For $\rho_0 = 0.17$ fm^{-3}, it has a value of about $P_F \approx 268$ MeV/c. In this sense, the distribution of the density is nonuniform in IQMD, which leads to the initial fluctuation. This makes possible the study of the initial fluctuation effects on the collective flow in IQMD.

III. ANISOTROPIC FLOW AND REACTION PLANE

During heavy ion collisions, the particle azimuthal distribution with respect to the reaction plane may not be isotropic, which is accustomed to be expanded in a Fourier series [32]:

$$E\frac{d^3N}{d^3p} = \frac{1}{2\pi}\frac{d^2N}{p_T dp_T dy}\left\{1 + \sum_{n=1}^{\infty} 2v_n \cos[n(\varphi - \psi^{\text{RP}})]\right\}, \tag{4}$$

where the $v_n = \langle\cos[n(\varphi_i - \psi^{\text{RP}})]\rangle$ coefficients are normally referred to as the nth collective flow or anisotropic flow [33] and ψ^{RP} is the reaction-plane angle. Ideally, the reaction plane is defined by the vector of the impact parameter and the beam direction. It is found that the magnitude of v_n is strongly correlated not only to the initial spatial eccentricity ε_n but also to the determination of the reaction plane.

A. Initial fluctuation and participant-plane method

The *initial fluctuation*, or the fluctuation of the initial collision geometry, originates from quantum fluctuations in the wave function of the projectile and target [1]. It affects both the orientation of the reaction plane and the value of the eccentricity. At the moment of maximum compression in the HIC, the overlap area is formed, which fluctuates from event to event. At this moment, the participant-plane angle can be defined as

$$\psi_n^{\text{PP}} = \frac{1}{n}\left[\arctan\frac{\langle r^2\sin(n\phi)\rangle}{\langle r^2\cos(n\phi)\rangle} + \pi\right], \tag{5}$$

where r and ϕ are the polar coordinate position of each nucleon and the average $\langle\ldots\rangle$ is density weighted in the initial state. The nth collective flow v_n with respect to participant plane is defined as

$$v_n = \left\langle\cos\left[n\left(\phi - \psi_n^{\text{PP}}\right)\right]\right\rangle. \tag{6}$$

The nth-order participant eccentricity calculated with respect to the participant plane is defined as

$$\varepsilon_n = \frac{\sqrt{\langle r^2\cos(n\phi)\rangle^2 + \langle r^2\sin(n\phi)\rangle^2}}{\langle r^2\rangle}. \tag{7}$$

In a previous study, it was found that the initial fluctuation causes the difference between the participant eccentricity and standard eccentricity of the smooth overlap distribution [34].

B. Event-plane method and resolution

As known in experiments, the reaction-plane angle cannot be directly measured, so the anisotropic flows v_n are measured with the event-plane method [35,36], which estimates the azimuthal angle of the reaction plane from the observed event plane determined from the collective flow itself. The event-plane angle is given as

$$\psi_n^{\text{EP}} = \arctan 2(Q_{n,y}, Q_{n,x})/n,$$

where

$$Q_{n,x} = \sum_i \omega_i \cos(n\varphi_i),$$
$$Q_{n,y} = \sum_i \omega_i \sin(n\varphi_i). \tag{8}$$

The above sum goes over all the particles used in the event-plane reconstruction. φ_i and ω_i are the azimuthal angle and weight for particle i. Since the optimal choice for ω_i is to approximate $v_n(p_T, y)$, the transverse momentum is a common choice as a weight [33]. The observed v_n measured with respect to the event plane is written as

$$v_n^{\rm obs} = \langle \cos[n(\varphi_i - \psi_n^{\rm EP})] \rangle. \tag{9}$$

Since finite multiplicity limits the estimation of the angle of the reaction plane, the v_n has to be corrected by the event-plane resolution for each harmonics, which is given by

$$\Re_n = \langle \cos[n(\psi_n^{\rm EP} - \psi^{\rm RP})] \rangle, \tag{10}$$

where the angle brackets mean an average over a large event sample. The event-plane resolution depends on the multiplicity of particles used to define the flow vector and the average flow of these particles via the resolution parameter [35–37]:

$$\Re_n(\chi) = \sqrt{\pi}/2 \exp(-\chi^2/2)[I_{(k-1)/2}(\chi^2/2) + I_{(k+1)/2}(\chi^2/2)], \tag{11}$$

where $\chi = v_n\sqrt{M}$, with M the multiplicity and $\boldsymbol{I_k}$ is the modified Bessel function of order k.

To calculate the resolution we divide the full events into two independent subevents of equal multiplicity [38]. The subevent resolution is defined as

$$\Re_{n,\rm sub} = \sqrt{\langle \cos[n(\psi_n^A - \psi_n^B)] \rangle}, \tag{12}$$

where A and B denote the two subgroups of particles. For the given $\Re_{n,\rm sub}$ the solution for χ in Eq. [11] is obtained by iteration. The full event-plane resolution is obtained by

$$\Re_{\rm full} = \Re(\sqrt{2}\chi_{\rm sub}). \tag{13}$$

The final collective flow with respect to the event plane is

$$v_n = \frac{v_n^{\rm obs}}{\Re_n}.$$

In the event-plane method, the event plane is calculated by the final momentum phase space. The flows extracted through this method may be affected by the following evolution of the reaction dynamics. In Ref. [5], it shows that in Au + Au collisions at $\sqrt{s_{NN}} = 200$ GeV from a multi-phase transport (AMPT) model the elliptic flow v_2 and the triangle flow v_3 with respect to the event plane are larger than those with respect to the participant plane. This illustrates that the evolution of the dynamics does influence the collective flow.

IV. RESULTS AND DISCUSSION

With the methods introduced above, we systematically study the collective flows. Centrality, the transverse component of the four velocity, and the rapidity-dependent behaviors for v_n are investigated. We stress the influence of initial fluctuations, which is for the first time considered in intermediate-energy HICs. The reaction system Au + Au is investigated to compare with the FOPI Collaboration experimental data [39].

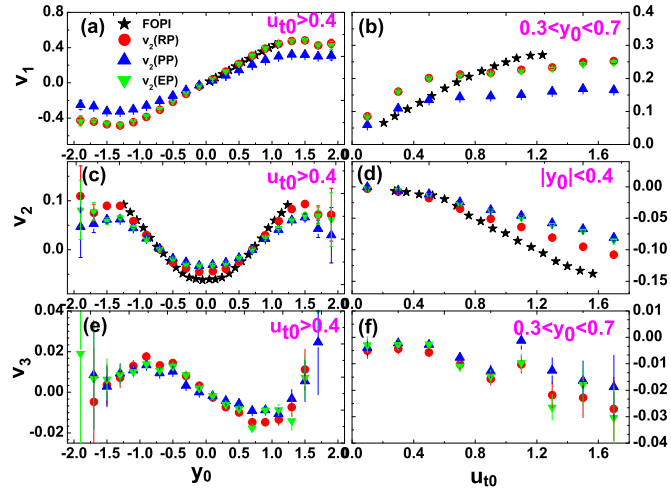

FIG. 1. (Color online) [(a), (b)] Comparison for directed flow v_1, [(c), (d)] elliptic flow v_2, and [(e), (f)] triangular flow v_3 with respect to reaction plane (red dots), participant plane (blue up triangles) and event plane (green down triangles) in Au + Au collisions at $E = 1A$ GeV and impact-parameter zone $0.25 < b_0 < 0.45$ from the IQMD simulation with the SM parameter. The black stars are the experimental data from FOPI (note the v_3 data of FOPI are not available). The y_0 dependence integrated over u_{t_0} but constrained to $u_{t_0} > 0.4$ is plotted in the left panel. The right panel shows theu_{t_0} dependence in the indicated y_0 region.

A. Flows with respect to different planes

Figure 1 shows y_0 (left panel) and u_{t_0} (right panel) dependencies of directed flow, elliptic flow, and triangular flow with respect to the *reaction plane* ($v_2^{\rm RP}$, i.e., the original Px-Pz plane in the IQMD model itself), *participant plane* ($v_2^{\rm PP}$), and *event plane* ($v_2^{\rm EP}$) together with the FOPI data [39], where $y_0 = y/y_p$ is the scaled rapidity (scaled to the projectile rapidity) and $u_{t_0} = u_t/u_p$ is the scaled transverse four-velocity. Note that, in the v_2 calculation, we applied the detector geometrical cut of the FOPI detector to make a quantitative comparison (the same for the following parts).

Before the analysis for the influence of initial fluctuations on the flows, we checked the impact of fluctuation on the particle spectrum itself. It is observed that there exists a quantitative difference between the average of the sum of p_x^2 and p_y^2 of particles event by event for different initial-fluctuation values. However, the effect of initial fluctuations is almost invisible to the single-particle spectrum itself. It is understandable that the initial fluctuation (x^2-y^2) in geometrical space have effects on momentum space (p_x^2-p_y^2) event by event, but the effect was washed out in the spectrum itself. This indicates that the effect of initial fluctuations on the spectrum is limited at the event-by-event level.

Now let us see the directed-flow case. It shows that the y_0 dependence of v_1 with respect to (w.r.t.) the participant

plane is weaker than that w.r.t. the reaction plane, and the shape of v_1 w.r.t. the event plane is steeper than that w.r.t. the participant plane. This means that the initial fluctuation decreases v_1; however, the evolution of dynamics recovers this effect so that $v_1^{\rm EP}$ is eventually similar to $v_1^{\rm RP}$. From the quantitative comparison with the data [39], the directed flow by either the reaction-plane method or by the event-plane method reasonably reproduces the v_1 data vs rapidity. However, the transverse-velocity dependence of the v_1 data cannot be perfectly fit by either simulation w.r.t various planes. In the low-u_{t_0} region, the v_1 simulation with the participant plane can describe more or less the data; however, the v_1 simulation with the reaction plane or event plane gives a close fit to the data.

Second, we move on the discussion on rapidity and transverse velocity dependencies of elliptic flow. A V-shape y_0 dependence [Fig. 1(c)] indicates that the proton favors in-plane emission ($v_2 > 0$) in projectile-like and target-like regions (larger rapidity) while the squeeze out ($v_2 < 0$) emission dominates in the overlapping region (midrapidity). From midrapidity to projectile-like or target-like rapidity, protons are dominantly emitted from out of plane to in plane, which is consistent with the decreasing of spectator shadowing. Transverse-velocity dependence [Fig. 1(d)] shows that, with increasing u_{t_0}, protons tend to be more squeeze-out emission, i.e., protons with higher transverse velocity can be easily ejected from the overlapping zone and more conically focused perpendicular to the beam axis.

From Figs. 1(c) and 1(d) one can see that v_2 w.r.t. the reaction plane is a little larger than that w.r.t. the participant plane, especially in higher velocity, which illustrates that the initial fluctuation weakens v_2. However, there is almost no discrepancy between v_2 w.r.t. the event plane and that w.r.t. the participant plane, which means that the dynamic evolution has little effect on v_2 in the present study. This phenomenon is different from what is known at RHIC energies, where the initial fluctuation enhances v_2 and the dynamic evolution further changes v_2 [5]. In the figure, the FOPI data are again plotted in order to check our model calculations. Although these three methods w.r.t. different planes for elliptic flow calculation do not give full quantitative agreements with the data, the trends of v_2 as functions of y_0 and u_{t_0} are similar to those of the data. Relatively, v_2 for the ideal reaction-plane method approaches the data nicely.

Third, we also study triangular flow v_3 with those three plane methods as functions of $y_0$and u_{t_0}, as shown in Figs. 1(e) and 1(f). They show that the initial fluctuation smooths the shape of the v_3 dependence on y_0 and u_{t_0}. Just like its effects on v_1, the initial fluctuation reduces the amplitude of v_3. It is also found that the magnitude of v_3 w.r.t. the event plane is not equal to that w.r.t. the reaction plane. However, all the magnitudes of v_3 calculated from various methods are limited only to within $\pm 2\%$. This is very different from the RHIC case, at which triangular flow originates mainly from the initial fluctuation.

B. Impact-parameter and beam-energy dependence

In Fig. 2, we show the centrality dependence of v_1 and v_2. Here the centrality is defined as a reduced impact parameter; namely b_0, which is the impact parameter normalized by the largest impact parameter of the system. Our calculation and FOPI data [39] results have similar values for all centralities. Both v_1 and v_2 reach their maximum at intermediate centrality ($0.45 < b_0 < 0.55$). The effect of initial fluctuation also shows the largest extent in the same centrality which can be seen from the increasing difference between $v_1^{\rm RP}$ and $v_1^{\rm PP}$ or between $v_2^{\rm RP}$ and $v_2^{\rm PP}$.

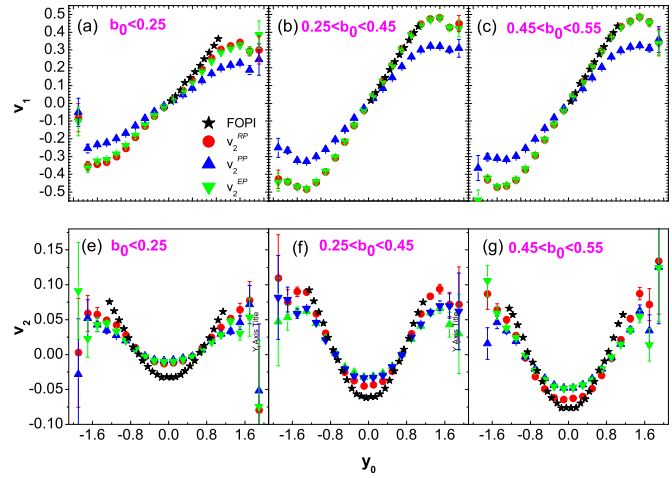

FIG. 2. (Color online) (upper panels) Rapidity dependence of directed flow v_1 and (lower panels) elliptic flow v_2 of protons in Au + Au collisions for different indicated centrality ranges. Transverse four-velocities u_{t_0} below 0.4 are cut off.

The average value of elliptic flow w.r.t. a participant plane, $v_2^{\rm PP}$, as a function of participant ε_2, at midrapidity ($|y_0| < 0.5$) is presented for $1A$ GeV Au + Au collisions in different impact-parameter regions in Fig. 3. It shows that the magnitude of $v_2^{\rm PP}$ is proportional to ε_2. Furthermore, the same slope holds for v_2 vs ε_2 except for a few of the largest ε_2 points. This indicates that elliptic anisotropy in initial-collision geometrical space leads to an elliptic anisotropy in particle production along the perpendicular direction in the overlapping participant zone. In previous studies at relativistic

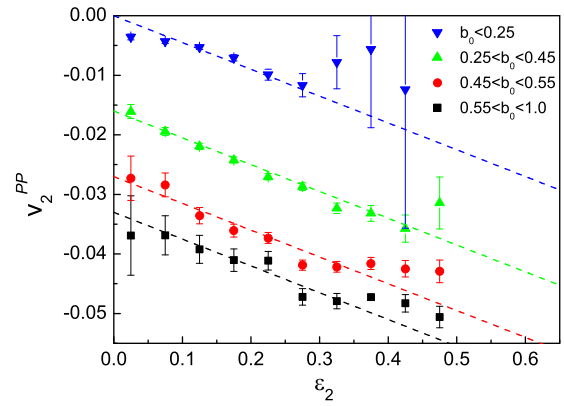

FIG. 3. (Color online) Average elliptic flow with respect to participant plane, $\langle v_2^{\rm PP}\rangle$, as a function of participant-plane eccentricity ε_2 at four given impact-parameter ranges for Au + Au collisions at $E = 1A$ GeV. The line describes a proportional relation of the absolute values of v_2 versus ε_2 with a slope of -0.045.

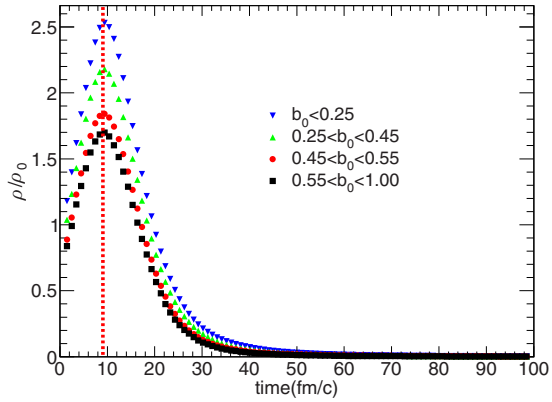

FIG. 4. (Color online) Average density evolutions with time at different impact parameters. A central sphere with radius 5 fm is selected to calculate the density. The maximum compression is around 9 fm/c.

energies, a proportional relationship between positive v_2 and ε_2 has also been demonstrated [5]. Here, a similar proportional trend is, for the first time, seen for the negative v_2 versus ε_2. It means that, under the shadowing effect, the squeeze-out emission becomes more conical when the the geometrical overlapping zone is more prolate. On the other hand, the absolute value of v_2 increases with impact parameter when ε_2 is 0, which can be attributed by the increasing shadowing effect at larger impact parameter [39].

In order to better understand the dynamical process, we consider the time evolutions of the density and ε_2. Before the collision ($t = 0$ fm/c), we set projectile and target at positions at $-r$ and r, respectively, in the beam direction in the center-of-mass system, where r is the radius of Au. Shown in Fig. 4 are the average density evolutions with time for $1A$ GeV Au + Au collisions in different impact-parameter regions. The system reaches their maximum densities near 9 fm/c, which are almost independent of impact parameter. Here, a central sphere with radius 5 fm is selected for the density calculation. We then calculate the average eccentricity of the system at this time, because the initial anisotropy changes little before the maximum compression stage. Shown in Fig. 5 are the time evolutions of

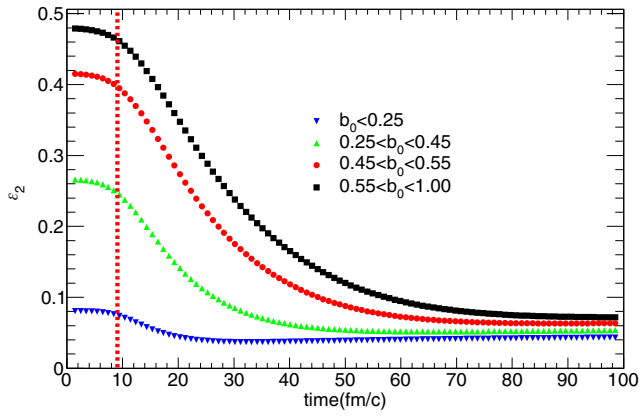

FIG. 5. (Color online) Average ε_2 evolutions with time at different impact parameters. The red dash line is around 9 fm/c.

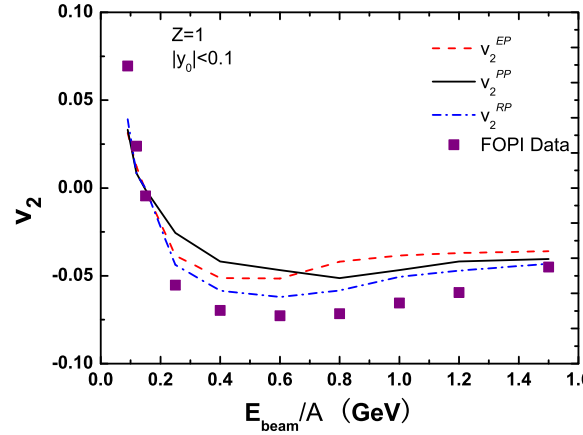

FIG. 6. (Color online) Elliptic flow with respect to different reaction planes as a function of beam energy for $Z = 1$ particles in Au + Au collisions at impact parameters of 5.5 fm $< b <$ 7.5 fm. The solid squares represent the experimental data [39] and different lines are for different reaction-plane methods.

the average eccentricity ε_2 of the system. It should be noted here that no special rapidity cut is applied here and the eccentricity ε_2 is defined according to Eq. (7). The eccentricity near 9 fm/c is chosen as the initial eccentricity, and its distribution reflects the initial fluctuation of the system. In this work, we do not focus on the effect from the distribution of the initial eccentricity, but the effect from the mean eccentricity. The initial fluctuation effect then comes most from the participant-plane angle at the event-by-event level, which is defined in Eq. (5).

Figure 6 shows a comparison of an excitation function of elliptic flow between IQMD calculation results and the FOPI experimental data [39]. Both IQMD calculation and experimental results show a transition energy from positive v_2 to negative v_2 around $0.2A$ GeV and a maximum squeeze-out flow around $0.5A$ GeV, and then decrease towards a transition to in-plane preferential emission at higher energies which are beyond our present energy points [40]. This energy dependence reflects that, in this energy regime, a competition results from a consequence of comparable spectator shadowing passing times and fireball expansion times [41]. At energies below $0.2A$ GeV, particles show positive elliptic flow, illustrating that a collective rotational behavior dominates [42,43]. Here, v_2 with the participant-plane method gives almost same values as those with the ideal reaction plane as well as event plane, which indicates that the initial geometrical fluctuation is actually not significant at lower beam energies. However, initial fluctuations makes the elliptic flow smaller in absolute value above $0.2A$ GeV where a squeeze-out mechanism dominates. As mentioned above, the squeeze out is an interplay of fireball expansion of participant and the shadowing effect of spectator. This is very different from those cases at RHIC and the CERN Large Hadron Collider (LHC) energy where stronger positive elliptic flow is mainly developed by the outward pressure in the isolated initial overlapping fireball. Here the initial fluctuation weakens the squeeze-out effect and reduces the elliptic flow, which indicates that the shadowing effect of spectators further quenches the anisotropy induced by the initial geometric fluctuation. In contrast, the initial

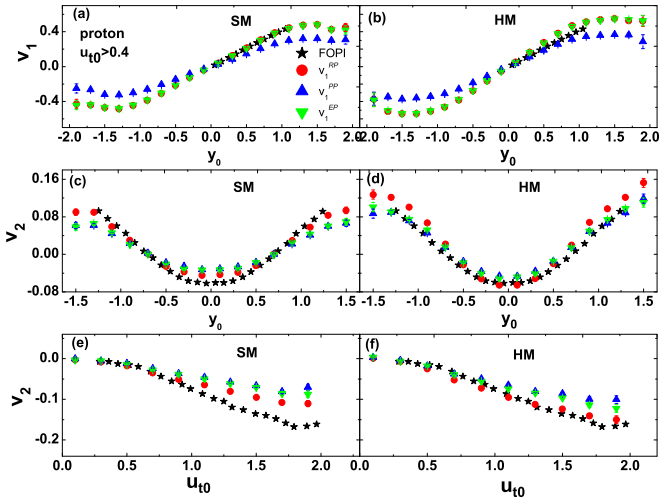

FIG. 7. (Color online) (left panels) Comparison between directed flow v_1 and elliptic flow v_2 from IQMD-SM simulation and (right panels) IQMD-HM simulation for Au + Au collisions at $E = 1A$ GeV in $0.25 < b_0 < 0.45$ centrality range. u_{t_0} below 0.4 are cut off.

fluctuation amplifies the positive elliptic flow at RHIC and LHC energies where the strong outward pressure further pushes initial fluctuation to become more anisotropic. In addition, the present calculations do not give full quantitative fits but underpredict the energy dependence of the squeeze-out flow even though the trend is well described, especially for the reaction-plane method. Of course, more calculations have been performed on the flow excitation function but no consistent agreement between data and calculations exists over all the energy range [41]. Hence, some space remains to improve the model. Here, in IQMD calculation, again we use the SM equation-of-state parameter.

C. Dependence on equation of state

We also compare the flows with different EOS parameters, i.e., with either the SM or the HM, as shown in Fig. 7. Our previous study on the particle spectrum has illustrated that the HM leads to a higher transverse momentum tail than the SM case [44]. From the viewpoint of the effects on flows, we can see the flows with the SM are smaller than those with HM, which is related to a higher transverse-momentum tail for HM [44]. And the effects of the initial fluctuation on v_1 and v_2 from SM are smaller than those from HM. We note that, for quantitative fits to the data, SM is better for v_1 with the reaction-plane method, but HM is better for the v_2 data with the same method. Hence, the model is not fully satisfied to describe the data, which remains the space to improve the model in some ways.

D. Scaling behavior of flows

In our previous theoretical study of low-energy flow, we found an approximate mass-number scaling that holds for directed flow as well as for elliptic flow of light nuclear fragments [45,46]. Later on, Oh and Ko also found a similar scaling of the nucleon number for deuteron at RHIC energies

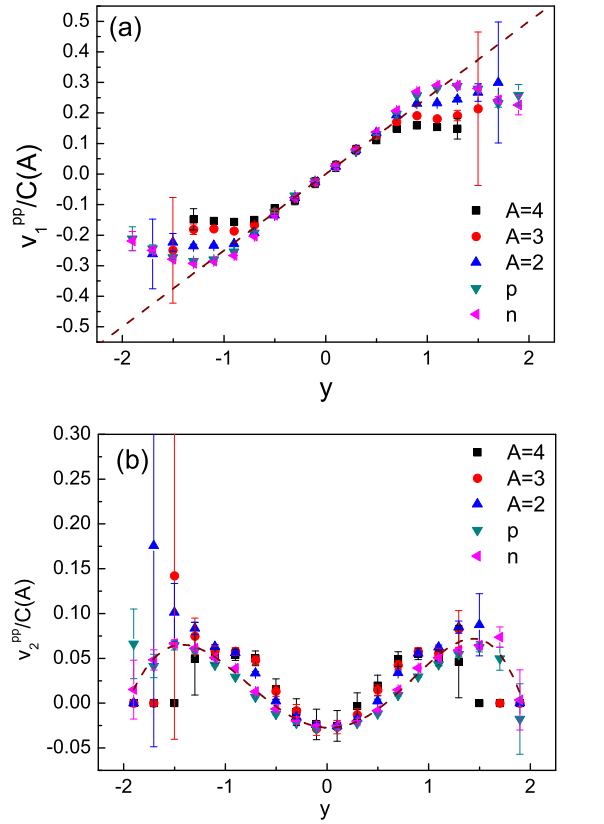

FIG. 8. (Color online) (a) Rapidity dependence of the $C(A)$ scaled v_1 and (b) v_2 for light particles of Au + Au at $1A$ GeV. Different symbols represent different light fragments. The lines are just to guide the eyes.

by using a dynamical model [47]. Figures 8(a) and 8(b) show the rapidity dependence of v_1 and v_2 scaled by a factor of $C(A)$ for light particles. Here $C(A) = \frac{5}{8}(A + \frac{3}{5})$ is a phenomenological function related to fragment mass number A, where the constant term can be seen to originate from the role of random motion and the term with mass number A reflects the collective motion which is proportional to mass. From Figs. 8(a) and 8(b) we can see for different fragments that the $C(A)$ scaled v_1 and v_2 can merge together, especially in the midrapidity region. This indicates that $C(A)$ scaling still works well for v_1 and v_2 after considering initial fluctuations. Note that the participant-plane method is adopted here to consider the effect of initial fluctuations.

In previous studies, the scaling behavior for v_4/v_2^2 and $v_3/(v_1 v_2)$ has been discussed in the hydrodynamical model and partonic transport model at RHIC energies [48,49] as well as in the quantum molecular dynamics model at low energy [46]. Here we also address these ratios as a function of p_T. Figures 9(a) and 9(b) show v_4/v_2^2 and $v_3/(v_1 v_2)$ for different light particles until mass number 4, respectively, in cases without or with considering initial fluctuation. Before the initial fluctuation is taken into account, v_4/v_2^2 and $v_3/(v_1 v_2)$ is about 0.5 and 0.6, respectively, independent of transverse momentum. This p_T-independent behavior indicates a kind of scaling. The value of 0.5 was predicted for v_4/v_2^2 by an ideal hydrodynamical model by assuming thermal equilibrium [49]

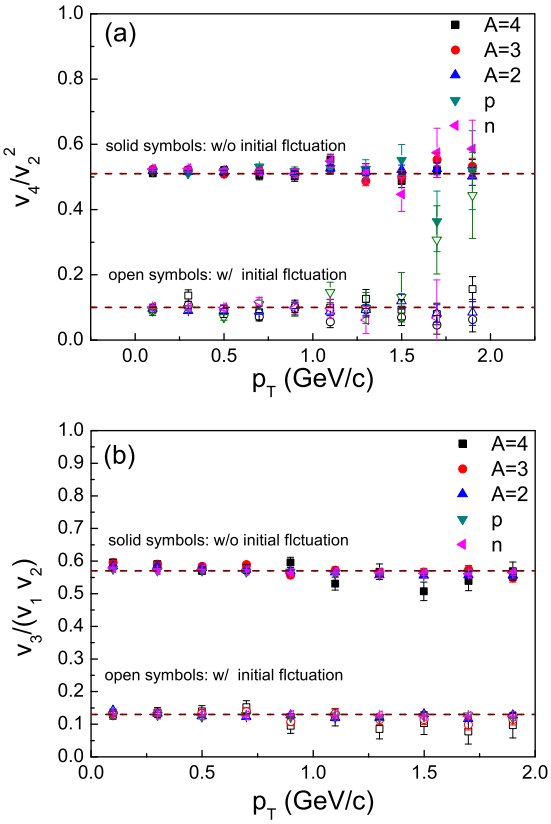

FIG. 9. (Color online) (a) Ratios of v_4/v_2^2 and (b) $v_3/(v_1 v_2)$ as a function of transverse momentum p_T for Au + Au at $1A$ GeV. Different symbols represent different fragments as indicted in inset. Solid symbols represent the ratios when the flows are calculated without initial fluctuation. Open symbols for the ratios when the initial fluctuation is taken into account for flow calculations. The lines are just to guide the eyes.

and the same ratio was also predicted by the quantum molecular dynamics model in our previous work on low-energy HICs [45] based on the nucleonic coalescence model. Here again, v_4/v_2^2 is around $1/2$ for $A = 1$ to 4 particles within IQMD model for $1A$ GeV Au + Au collision, which means the nucleonic coalescence model can explain the ratio. However, this ratio dramatically decreases after the initial fluctuation is taken into account in our flow calculations, eg., v_4/v_2^2 is only around 0.1. This behavior seems in contrast with the phenomenon in relativistic heavy ion collisions where the high value of v_4/v_2^2 seen experimentally is argued mostly by invoking elliptic flow fluctuations [50]. However, the ratios for different light particles still remain the same as well as being independent of transverse momentum, i.e., the scaling behavior does not break. Similarly, $v_3/(v_1 v_2)$ shows a constant value around 0.6 before the initial fluctuation is considered, but it decreases to around 0.12 when the initial fluctuation is taken into account. The decreased ratios indicate that the higher harmonic flow is quenched more strongly due to the initial fluctuation. This is similar to viscous damping for higher harmonic flows [5].

V. SUMMARY

We analyzed the flows as functions of rapidity, transverse four-velocity, centrality, and beam energy for Au + Au collisions at $1A$ GeV to investigate the effect of the initial fluctuation on flows. We emphasize that this is the first check of the initial-fluctuation effect on the squeeze-out emission. Quantitative comparison of the flows w.r.t. the participant plane is made with the experimental method (event-plane method) to investigate the effect of evolution of dynamics. In addition, we compare the flows with the experimental data from the FOPI Collaboration. We find that the initial participant fluctuation has indeed some effects on the flows. However, in contrast with HICs in the ultrarelativistic region, the initial fluctuation weakens the squeeze-out flow, which indicates that the anisotropy due to initial fluctuations was quenched to some extent by the spectator-shadowing effect. In addition, squeeze-out flow is also proportional to initial eccentricity, indicating that squeeze-out essentially develops from the initial overlapping region. A quantitative comparison with the excitation function of v_2 shows that our simulation data are smaller than the experimental data even though the trend is very close, which may be caused by two reasons: One is the variation of physical parameters (like the ground-state densities, interaction ranges) whose precise values are not known; the other is that the complicated input parameters such as the EOS, in-medium cross section, etc. are not well known.

In addition, the flow-scaling behaviors for different light fragments are also checked in the present simulation. It is found that the v_1 and v_2 of different fragments can be scaled by a function of mass number plus a constant term even the initial fluctuation has been taken into account. The ratios v_4/v_2^2 and $v_3/(v_1 v_2)$ demonstrate a constant value which is independent of transverse momentum when the initial fluctuation is not considered. The value of $1/2$ for v_4/v_2^2 indicates that the nucleonic coalescence model can explain the fragment flows. However, when the initial fluctuation is considered, the ratios still have constant values but are much smaller than the former. This indicates that, even though the scaling behavior is not broken, higher harmonic flows will be strongly quenched by the initial fluctuation in an effect similar to viscous damping.

ACKNOWLEDGMENTS

We thank Dr. Lixin Han and Dr. Zhigang Xiao for helpful discussion. This work was supported in part by the Major State Basic Research Development Program of China under Contract No. 2014CB845401 and the National Natural Science Foundation of China under Contracts No. 11035009 and No. 11220101005.

[1] B. Alver and G. Roland, Phys. Rev. C **81**, 054905 (2010).

[2] B. Alver, B. Back, M. Baker, M. Ballintijn, D. Barton *et al.*, Phys. Rev. C **77**, 014906 (2008).

[3] J. Xu and C. M. Ko, Phys. Rev. C **83**, 021903 (2011).
[4] G. L. Ma and X. N. Wang, Phys. Rev. Lett. **106**, 162301 (2011).
[5] L. X. Han, G. L. Ma, Y. G. Ma, X. Z. Cai, J. H. Chen, S. Zhang, and C. Zhong, Phys. Rev. C **84**, 064907 (2011).
[6] O. Socolowski, Jr., F. Grassi, Y. Hama, and T. Kodama, Phys. Rev. Lett. **93**, 182301 (2004).
[7] R. Andrade, F. Grassi, Y. Hama, T. Kodama, and O. Socolowski, Jr., Phys. Rev. Lett. **97**, 202302 (2006).
[8] R. P. G. Andrade, F. Grassi, Y. Hama, T. Kodama, and W. L. Qian, Phys. Rev. Lett. **101**, 112301 (2008).
[9] J. Takahashi, B. Tavares, W. Qian, R. Andrade, F. Grassi *et al.*, Phys. Rev. Lett. **103**, 242301 (2009).
[10] X. Zhu, M. Bleicher, and H. Stöecker, Phys. Rev. C **72**, 064911 (2005).
[11] H. Petersen, C. Coleman-Smith, S. A. Bass, and R. Wolpert, J. Phys. G **38**, 045102 (2011).
[12] L. Ma, G. L. Ma, and Y. G. Ma, Phys. Rev. C **89**, 044907 (2014).
[13] Y. Hu, Z. Q. Su, and W. N. Zhang, Nucl. Sci. Tech. **24**, 050522 (2013).
[14] B. Schenke, S. Jeon, and C. Gale, Phys. Rev. Lett. **106**, 042301 (2011).
[15] L. Adamczyk *et al.* (STAR Collaboration), Phys. Rev. Lett. **112**, 032302 (2014).
[16] C. M. Ko, L. W. Chen, V. Greco, F. Li, Z. W. Lin, S. Plumari, T. Song, and J. Xu, Nucl. Sci. Tech. **24**, 050525 (2013); J. Xu, T. Song, C. M. Ko, and F. Li, Phys. Rev. Lett. **112**, 012301 (2014).
[17] J. Tian, J. H. Chen, Y. G. Ma, X. Z. Cai, F. Jin, G. L. Ma, S. Zhang, and C. Zhong, Phys. Rev. C **79**, 067901 (2009).
[18] F. M. Liu, Nucl. Sci. Tech. **24**, 050524 (2013).
[19] J. Wang, Y. G. Ma, G. Q. Zhang, D. Q. Fang, L. X. Han, and W. Q. Shen, Nucl. Sci. Tech. **24**, 030501 (2013).
[20] J. Aichelin, Phys. Rep. **202**, 233 (1991).
[21] H. Kruse, B. V. Jacak, and H. Stöecker, Phys. Rev. Lett. **54**, 289 (1985).
[22] C. Hartnack, R. K. Puri, J. Aichelin, J. Konopka, S. Bass *et al.*, Eur. Phys. J. A **1**, 151 (1998).
[23] T. Maruyama, K. Niita, and A. Iwamoto, Phys. Rev. C **53**, 297 (1996).
[24] W. B. He, Y. G. Ma, X. G. Cao, X. Z. Cai, and G. Q. Zhang, Phys. Rev. Lett. **113**, 032506 (2014).
[25] Q. Li, C. Shen, C. Guo, Y. Wang, Z. Li, J. Lukasik, and W. Trautmann, Phys. Rev. C **83**, 044617 (2011).
[26] G. Q. Zhang, Y. G. Ma, X. G. Cao, C. L. Zhou, X. Z. Cai *et al.*, Phys. Rev. C **84**, 034612 (2011).
[27] C. Tao, Y. G. Ma, G. Q. Zhang, X. G. Cao, D. Q. Fang, and H. W. Wang, Nucl. Sci. Tech. **24**, 030502 (2013); Y. X. Zhang, Z. X. Li, K. Zhao, H. Liu, and M. Tsang, *ibid.* **24**, 050503 (2013).
[28] C. Grégoire, B. Remaud, F. Sébille, L. Vinet, and Y. Raffray, Nucl. Phys. A **465**, 317 (1987).
[29] P.-B. Gossiaux, D. Keane, S. Wang, and J. Aichelin, Phys. Rev. C **51**, 3357 (1995).
[30] J. Aichelin, A. Rosenhauer, G. Peilert, H. Stoecker, and W. Greiner, Phys. Rev. Lett. **58**, 1926 (1987).
[31] S. Voloshin and Y. Zhang, Z. Phys. C: Part. Fields **70**, 665 (1996).
[32] S. A. Voloshin, A. M. Poskanzer, and R. Snellings, in *Relativistic Heavy Ion Physics*, edited by R. Stock (Springer, Berlin, Heidelberg, 2010), Vol. 23, pp. 293–333.
[33] S. Manly *et al.* (PHOBOS Collaboration), Nucl. Phys. A **774**, 523 (2006).
[34] J. Barrette *et al.* (E877 Collaboration) Phys. Rev. Lett. **73**, 2532 (1994).
[35] A. M. Poskanzer and S. A. Voloshin, Phys. Rev. C **58**, 1671 (1998).
[36] J.-Y. Ollitrault, Nucl. Phys. A **638**, 195c (1998).
[37] P. Danielewicz and G. Odyniec, Phys. Lett. B **157**, 146 (1985).
[38] J.-Y. Ollitrault, Phys. Rev. D **48**, 1132 (1993).
[39] W. Reisdorf *et al.* (FOPI Collaboration), Nucl. Phys. A **876**, 1 (2012).
[40] C. Pinkenburg *et al.*, Phys. Rev. Lett. **83**, 1295 (1999).
[41] A. Andronic *et al.* (FOPI Collaboration), Phys. Lett. B **612**, 173 (2005).
[42] Y. G. Ma, W. Q. Shen, J. Feng, and Y. Q. Ma, Phys. Rev. C **48**, R1492 (1993).
[43] Y. G. Ma and W. Q. Shen, Phys. Rev. C **51**, 3256 (1995).
[44] M. Lv, Y. G. Ma, G. Q. Zhang, J. H. Chen, and D. Q. Fang, Phys. Lett. B **733**, 105 (2014).
[45] T. Z. Yan, Y. G. Ma, X. Z. Cai, J. G. Chen, D. Q. Fang, W. Guo, C. W. Ma, E. J. Ma, W. Q. Shen, W. D. Tian, and K. Wang, Phys. Lett. B **638**, 50 (2006).
[46] T. Z. Yan, Y. G. Ma *et al.*, Chin. Phys. Lett. **24**, 3388 (2007); Chin. Phys. (Beijing, China) **16**, 2676 (2007).
[47] Yongseok Oh and Che Ming Ko, Phys. Rev. C **76**, 054910 (2007).
[48] P. F. Kolb, L. W. Chen, V. Greco, and C. M. Ko, Phys. Rev. C **69**, 051901(R) (2004).
[49] N. Borghini and J.-Y. Ollitrault, Phys. Lett. B **642**, 227 (2006).
[50] C. Gombeaud and J.-Y. Ollitrault, Phys. Rev. C **81**, 014901 (2010).